MicroRNA-155-5p affects regulatory T cell activation and immunosuppressive function by targeting BCL10 in myasthenia gravis

JING SUN[1], MENGJIAO SUN[1], XIAOLING LI[1], QINFANG XIE[1], WENJING ZHANG[2] and MANXIA WANG[1]

[1]Department of Neurology, Lanzhou University Second Hospital, Lanzhou, Gansu 730030;
[2]Department of Neurology, Qinghai Provincial People's Hospital, Xining, Qinghai 810007, P.R. China

Received February 13, 2023; Accepted October 20, 2023

DOI: 10.3892/etm.2023.12293

Abstract. The imbalance in immune homeostasis plays a crucial role in the pathogenesis of myasthenia gravis (MG). MicroRNAs (miRs) have been identified as key regulators of immune homeostasis. B-cell lymphoma/leukemia 10 (BCL10) has been implicated in the activation and suppressive function of regulatory T cells (Tregs). This study aimed to investigate the potential role of miR-155-5p in modulating the activation and function of Tregs in MG. To achieve this objective, blood samples were collected from MG patients to assess the expression levels of miR-155-5p and BCL10, as well as the proportion of circulating Tregs, in comparison to healthy controls. The correlation between miR-155-5p and BCL10 levels was evaluated in human samples. The expression levels of miR-155-5p and the numbers of circulating Tregs were also examined in an animal model of experimental autoimmune MG (EAMG). A dual-luciferase reporter assay was used to verify whether miR-155-5p can target BCL10. To determine the regulatory function of BCL10 in Tregs, $CD4^+$ $CD25^+$ Tregs were transfected with either small interfering-BCL10 or miR-155-5p inhibitor, and the expression levels of the anti-inflammatory cytokine IL-10 and transcription factors Foxp3, TGF-β1, CTLA4, and ICOS were measured. The results demonstrated that the expression level of miR-155-5p was significantly higher in patients with MG compared with that in healthy controls, whereas the expression level of BCL10 was significantly decreased in patients with MG. Furthermore, there was a significant negative correlation between the expression levels of miR-155-5p and BCL10. The number of circulating Tregs was significantly reduced in patients with MG and in the spleen of rats with EAMG compared with that in the corresponding control groups. The dual-luciferase reporter assay demonstrated that miR-155-5p could target BCL10. The Tregs transfected with si-BCL10 demonstrated significant decreases in the protein levels of TGF-β1 and IL-10, as well as in the mRNA expression levels of Foxp3, TGF-β1, CTLA-4 and ICOS. Conversely, the Tregs transfected with the miR-155-5p inhibitor exhibited a substantial increase in these protein and mRNA expression levels compared with their respective control groups. Furthermore, the knockdown of BCL10 exhibited a decline in the suppressive efficacy of Tregs on the proliferation of $CD4^+$ T cells. Conversely, the suppression of miR-155-5p expression attenuated the inhibition of the BCL10 gene, potentially causing an indirect influence on the suppressive capability of Tregs on the proliferation of $CD4^+$ T cells. BCL10 was thus found to contribute to the activation and immunosuppressive function of Tregs. In summary, the present study demonstrated that miR-155-5p inhibited the activation and immunosuppressive function of Tregs by targeting BCL10, which may be used as a future potential target for the treatment of MG.

Introduction

Myasthenia gravis (MG) is an antibody-mediated neurological autoimmune disorder, caused by transmission defects in the neuromuscular junction (1). The incidence rate of this disease ranges from 4.1 to 30 cases per million person-years, with a prevalence rate spanning from 150 to 200 cases per million individuals (2). It has been reported that MG results from a loss of self-tolerance, which allows auto-reactive lymphocytes to develop. There are a number of mechanisms that may contribute to compromised self-tolerance in MG, one of which is a quantitative, functional and migratory deficit in regulatory T cells (Tregs) (3).

Previous studies have focused on recognizing antigen epitopes, assisting B cells to differentiate and mature into plasma cells to produce antibodies and secrete cytokines of different T-cell subsets during MG progression, and their contributions to immune activation and autoimmunity (4,5). It has been reported that Treg dysfunction contributes to the pathogenesis of MG (6,7). However, data are conflicting regarding whether

Correspondence to: Professor Manxia Wang or Dr Jing Sun, Department of Neurology, Lanzhou University Second Hospital, 82 Cuiyingmen, Chengguan, Lanzhou, Gansu 730030, P.R. China
E-mail: wmx322@aliyun.com
E-mail: sunjing1221@163.com

Key words: myasthenia gravis, microRNA-155-5p, B-cell lymphoma/leukemia 10, regulatory T cells

reduced Treg numbers contribute to disease pathogenesis (8,9). Treg suppressive function and effector T cell numbers from patients with MG are both observed as abnormalities *in vivo* studies (10). Tregs are a subgroup of T cells that regulate autoimmune reactivity by inhibiting the function of other effector T cells and antigen-presenting cells (11). Tregs release multiple immunoinhibitory cytokines, such as transforming growth factor-β1 (TGF-β1) and interleukin-10 (IL-10) (11). The immunomodulatory properties of Tregs are controlled by the expression of fork-head box protein 3 (Foxp3) (12). Inhibition of the suppressive abilities of Tregs may lead to the increased production of pro-inflammatory cytokines, such as IL-6, IL-17 and IFN-γ, as well as in the activation of autoantibody-producing B cells (13).

MicroRNAs (miRNAs/miRs) are small, non-coding RNAs that regulate immune function and homeostasis (14-17). Although these previous studies have provided considerable insight into the role of miRNAs in immune homeostasis, their direct targets remain to be fully elucidated, particularly in Tregs. miR-155-5p has been shown to regulate the differentiation of lymphocyte subsets, such as B cells and $CD8^+$ and $CD4^+$ T cells, including T-helper type and Tregs (18). Previous studies have demonstrated that miRNAs are involved in the pathogenesis of MG (4,19), and the expression level of miR-155 is significantly increased in peripheral blood mononuclear cells (PBMCs) of patients with MG (20). However, to the best of our knowledge, a direct link between miR-155 dysregulation and impaired Treg induction in the context of MG onset has not been reported to date.

B-cell lymphoma/leukemia 10 (BCL10) is an intracellular signaling protein that serves a role in T cell receptor-induced NF-κB activation in Tregs and participates in the production of Treg effectors under homeostatic conditions (21). Previous animal studies reported that BCL10 regulates the development and function of Tregs (21,22) and can be targeted by miR-155-5p (23). However, whether miR-155-5p and BCL10 contribute to the pathological mechanisms of MG remains unknown. Thus, the present study aimed to explore whether miR-155-5p could target BCL10 and regulate the function of Tregs in MG.

Materials and methods

Study subjects. A total of 18 patients with MG were recruited from the Department of Neurology at the Second Hospital of Lanzhou University (Lanzhou, China). The inclusion criteria were as follows: i) Meeting the diagnostic criteria for MG (24); ii) detection of AChR antibody in all collected samples; and iii) Myasthenia Gravis Foundation of America classification of I to IV (25). The exclusion criteria encompassed individuals with concomitant cognitive impairment, other autoimmune diseases, malignant tumors, liver and kidney insufficiency, and coagulation disorders. A total of 15 healthy controls were also recruited from the Physical Examination Center of the Second Hospital of Lanzhou University. The inclusion criteria for these controls were as follows: i) Absence of any disease status upon physical examination; and ii) matching the sex and age of the patients with MG. The quantitative MG (QMG) score (26) was measured by two researchers who were blinded to the experimental groups. All patients with MG and healthy individuals were recruited between May 2021 and May 2022. The study was approved by the Ethics Committee of Lanzhou University Second Hospital (approval no. 2021A-445; Lanzhou, China), and all samples were collected after obtaining written informed consent from the participants. Subsequently, fresh blood samples were collected from 18 patients diagnosed with MG and 15 healthy controls, which were then utilized for reverse transcription-quantitative (RT-q)PCR and flow cytometry analysis. The baseline characteristics of the study population, including age and sex distribution, and the demographic characteristics of the patients with MG are presented in Tables I and II, respectively.

Establishment and clinical evaluation of acetylcholine receptor (AChR)-induced experimental autoimmune MG (EAMG). A total of 16 female Lewis rats (7 weeks old; 170±2 g; Beijing Vital River Laboratory Animal Technology Co., Ltd.) were bred under the following pathogen-free conditions: Light/dark cycle, 12/12 h; temperature, 21-22˚C; humidity, 55±5%; and water and food intake, *ad libitum*. Autoimmunity was induced by injecting the R97-116 peptide (sequence, DGDFAIVKFTKVLLDYTGHI; CSBio). In torpedo and rat receptors, 16 of the 20 residues of the R97-116 sequence are identical, and the R97-116 polypeptide is a synthetic peptide with 80% homology to the AChR-α subunit. Baggi *et al* (27) previously reported that induction of EAMG in rats using the R97-116 peptide resulted in a high rate of success. Clinical scores, clinical incidence, body weight measurement, AChR-specific antibody detection and muscle AChR detection were employed to illustrate the effective induction of experimental autoimmune myasthenia gravis (EAMG) following AChR immunization. Additionally, the EAMG rat model exhibited hunched posture, muscle strength, and fatigability, which closely mirrored the symptoms observed in clinical MG patients. Briefly, the animals used in the present study were anesthetized via intraperitoneal injection of pentobarbital sodium (50 mg/kg) prior to subcutaneous immunization. Each animal was injected with a total volume of 200 μl inoculum containing R97-116 peptide (50 μg), emulsified in complete Freund's adjuvant (CFA; MilliporeSigma). On day 11 post-injection, all rats were boosted by injecting R97-116 peptide emulsified in incomplete Freund's adjuvant (IFA; MilliporeSigma) at four well-separated sites on the back of the animals (50 μg/rat). The control rats were immunized with subcutaneous injections of CFA and IFA. Animals were euthanized via an intraperitoneal injection of sodium pentobarbital (200 mg/kg) (28). All animal experiments were approved by the Animal Care and Use Committee of Lanzhou University Second Hospital (approval no. 2021A-319; Lanzhou, China).

The weight of the rats, Lennon scores and the levels of anti-AChR antibody in the serum were used to assess whether the EAMG animal model was successfully established. Briefly, all rats were weighed and scored at the beginning of the experiment and at least twice a week until the end of the experiment on day 45. The Lennon score was evaluated according to previously described criteria (29). Disease severity was graded as follows: 0, normal; 1, mildly decreased activity, weak grip and fatigable; 2, weakness, hunched posture at rest, decreased

Table I. Baseline characteristics of the study population.

Characteristics	Patients with MG (n=18)	Healthy controls (n=15)	P-value
Age, years	49.20±3.50	50.22±3.69	0.8440
Female sex, n (%)	11 (18)	9 (15)	>0.9999
BMI, kg/m^2	23.25±1.14	20.84±0.36	0.0725

body weight and tremor; 3, severe generalized weakness, a marked decrease in body weight and moribund; and 4, death. Rats with intermediate signs were assigned grades of 0.5, 1.5, 2.5 or 3.5, respectively.

Anti-AChR antibodies. The absolute anti-AChR antibody levels in rats with EAMG were evaluated using an ELISA kit (cat. no. EK-R31157; Shanghai Enzyme Research Biotechnology Co., Ltd.). After administering anesthesia to the rats, a fresh blood sample of 500 μl was obtained from the heart and subsequently underwent centrifugation at 1,000 x g for 10 min at 4˚C to isolate the serum. The obtained serum was then diluted using a diluent comprising 1% phosphate-buffered saline (PBS; cat. no. P1022; Beijing Solarbio Science & Technology Co., Ltd.) and 2% fetal bovine serum (FBS; cat. no. 10099158; Gibco). This diluted serum was added to the assay plate at a volume of 100 μl per well and incubated at 37˚C for 90 min. Subsequently, the liquid within the wells was discarded and incubated with 100 μl of biotin-labeled antibodies for 30 min at 37˚C. Following this, the assay plate underwent three cycles of washing, after which 100 μl of streptavidin-HRP working solution was added and incubated at 37˚C for 30 min. The plate was then washed five times before the addition of 90 μl of the chromogenic reagent tetramethylbenzidine to each well, and incubated at 37˚C for 15 min in the dark. Finally, the reactions were terminated by adding 100 μl of the stop solution (1M H3PO4). The optical density of the test samples and standard was measured using a Multiskan™ FC microplate reader (Thermo Fisher Scientific, Inc.) at 450 nm.

Flow cytometry. To determine the proportion of CD4$^+$ CD25^{hi} CD127^{low} Tregs in the peripheral blood of patients with MG and the proportion of CD4$^+$ CD25$^+$ Foxp3$^+$ Tregs in splenic lymphocytes of EAMG rats, flow cytometry guidelines were followed (30). Briefly, 100 μl of freshly collected peripheral blood was added to a 1.5-ml centrifuge tube, followed by 300 μl red cell lysis buffer (C3702; Beyotime Institute of Biotechnology), mixed thoroughly, and incubated in the dark at RT for 5 min. Subsequently, 5 μl human TruStain FcX Fc receptor blocking solution (cat. no. 422301; BioLegend, Inc.) was added to the 1x10^6 cells/sample and incubated at RT in the dark for 10 min, and centrifuged at 500 x g for 5 min at RT. Subsequently, the samples were stained with fluorochrome-conjugated antibodies against surface markers FITC anti-human CD4 (0.5 mg/ml; cat. no. 300505; BioLegend, Inc.), phycoerythrin (PE) anti-human CD25 (0.5 mg/ml; cat. no. 302605; BioLegend, Inc.) and allophycocyanin (APC) anti-human CD127 (0.2 mg/ml; cat. no. 351315; BioLegend, Inc.) antibodies, and incubated in the dark at 4˚C for 30 min. Rat spleen mononuclear cells were isolated by density gradient centrifugation and counted at 1x10^6 cells/100 μl per tube, then 5 μl 2% BSA (cat. no. A8020; Beijing Solarbio Science & Technology Co., Ltd.) was added to 1x10^6 cells/tube and incubated at RT in the dark for 15 min to block non-specific staining. The mixture was centrifuged at 450 x g for 5 min at RT, then 1x10^6 cells/samples were incubated with FITC anti-rat CD4 (0.5 mg/ml; cat. no. 201505; BioLegend, Inc.) and PE anti-rat CD25 (0.2 mg/ml; cat. no. 202105; BioLegend, Inc.) antibodies at 4˚C in the dark for 30 min. Following fixation for 20 min and permeabilization for 15 min at RT using FOXP3 Fix/Perm Buffer Set (cat. no. 421403; BioLegend, Inc.), cells were stained with APC anti-rat Foxp3 antibodies (0.2 mg/ml; cat. no. 77-5775-40; eBioscience; Thermo Fisher Scientific, Inc.) at RT in the dark for 30 min. Mouse IgG1 κ labeled with the same fluorescence as the flow antibody, was set as a negative control (cat. no. F11IG101, 0.2 mg/ml; cat. no. F11IG103; 0.2 mg/ml; cat. no. F11IG102, 0.2 mg/ml; Hangzhou MULTISCIENCES Co., Ltd.). Stained cells were counted using a BD FACSCanto™ flow cytometer (BD Biosciences) and analyzed using FlowJo™ software (version 10.8.1; FlowJo LLC).

Dual-luciferase reporter assay. Bioinformatics analysis was performed to predict the potential targets of miR-155-5p using the TargetScan 8.0 software (https://www.targetscan.org/). To verify whether BCL10 and miR-155-5p could bind, the human BCL10 3'-untranslated region (UTR) sequence that was predicted to interact with the miR-155-5p seed sequence was mutated (Mut, the putative binding site was changed from 5'-AGCATTAA-3' to 5'-TCGAAATT-3'; Shanghai GenePharma Co., Ltd.). Human BCL10-wild-type (WT) and BCL10-Mut 3'-UTRs were cloned into the pmirGLO (Shanghai GenePharma Co., Ltd.) vector containing both *Renilla* and firefly luciferase. 293T cells (The Cell Bank of Type Culture Collection of the Chinese Academy of Sciences; cultured in DMEM (cat. no. 31600034; Gibco; Thermo Fisher Scientific, Inc.) with 10% FBS (Gibco; Thermo Fisher Scientific, Inc.) at 37˚C with 5% CO_2 were seeded in 12-well plates at a concentration of 5x10^5 cells/well. miR-155-5p mimics or mimics negative control (NC) (20 μM; Shanghai GenePharma Co., Ltd.; Table III) and 1.6 μg of the aforementioned luciferase reporter plasmid were co-transfected into 293T cells using the GP-transfect-Mate reagent (Shanghai GenePharma Co., Ltd.). After 48 h, the cells were collected for detection of the luciferase activity using the Dual-Luciferase® Reporter Assay System (Promega Corporation). The ratio of *Renilla* luciferase to firefly luciferase activity was calculated. All experiments were performed in duplicate.

Transfection of miR-155-5p mimics and miR-155-5p inhibitor in Jurkat cells. In the present study, the selection of miR-155-5p mimics and miR-155-5p inhibitor as exogenous biomacromolecules was based on their characteristics, namely their ability to be transfected into cells solely through the use of transfection reagents, thereby eliminating the need for intricate vector construction and concerns regarding viral protection. miRNA inhibitors, which are chemically modified oligonucleotides

Table II. Demographic characteristics of patients with MG.

Patient	Age at onset, years	Sex, M/F	Disease duration, months	MGFA clinical classification	QMG score	Abnormalities of the thymus	Acetylcholine receptor antibody levels (nmol/l)
MG1	32	F	6.0	I	-	Thymoma	~
MG2	55	M	1.0	I	13	/	17.12
MG3	52	F	2.5	IIIa	27	/	8.34
MG4	34	M	2.0	I	-	Thymic hyperplasia	~
MG5	46	F	1.0	I	18	/	~
MG6	39	M	3.0	IIa	15	/	22.67
MG7	43	M	36.0	IIIa	5	Thymic hyperplasia	117.60
MG8	55	M	66.0	IIa	-	/	11.68
MG9	72	F	24.0	I	28	Thymoma	~
MG10	36	F	6.0	IIb	19	/	14.27
MG11	24	M	3.0	I	17	Thymic hyperplasia	~
MG12	63	M	0.5	I	7	/	~
MG13	47	F	6.0	IIIa	22	Thymic hyperplasia	32.18
MG14	12	F	600.0	IIa	29	/	45.26
MG15	59	M	1.5	IVb	21	Thymoma	39.26
MG16	17	F	1.0	IIb	11	/	~
MG17	45	M	132.0	IIa	-	Thymic hyperplasia	26.67
MG18	56	F	12.0	I	15	/	4.58

MG, myasthenia gravis; MGFA, Myasthenia Gravis Foundation of America; QMG, quantitative MG; M, male; F, female; -, not known; /, normal; ~, AChR Ab negative.

that exhibit complete complementarity to endogenous mature miRNA, were chosen due to their ability to inhibit the functions of target miRNAs effectively (31). miR-155-5p mimics, inhibitor, and NC oligonucleotides (Table III) were purchased from Shanghai GenePharma Co., Ltd. Jurkat T Cells (Procell Life Science & Technology Co., Ltd.) were transfected with the corresponding oligonucleotides using Entranster™-R4000 (Engreen Biosystem, Co., Ltd.) according to the manufacturer's instructions. Cells were seeded in 24-well plates 1 day prior to the experiment. Jurkat T cells were cultured in RPMI-1640 medium (Gibco; Thermo Fisher Scientific, Inc.) with 10% FCS (Gibco; Thermo Fisher Scientific, Inc.), 1% L-glutamine (MilliporeSigma), 1% sodium pyruvate, 1% non-essential amino acids, $2x10^{-5}$ M 2-mercaptoethanol (Amresco, LLC) and 1% penicillin-streptomycin (Gibco; Thermo Fisher Scientific, Inc.). Cells in the logarithmic growth phase were used, with a total of $2x10^5$ cells/well used for transfection. A total of 0.67 μg (50 pmol) miR-155-5p mimics, miR-155-5p inhibitor or NC oligonucleotides were mixed with 25 μl serum-free RPMI-1640. Additionally, a 25 μl Entranster™-R4000 solution was prepared by mixing 1 μl Entranster™-R4000 with 24 μl serum-free RPMI-1640. Entranster™-R4000 and miRNA solutions were mixed and incubated for 15 min at RT. Subsequently, the 50-μl transfection solution was added to the cells along with 0.45 ml complete RPMI-1640 medium as aforementioned, and incubated at 37˚C. After a transfection period lasting 6 h, the cells were found to be in a favorable condition. Consequently, the cells were cultured for 48 h before the initiation of subsequent experiments.

Isolation of $CD4^+$ T cells and $CD4^+$ $CD25^+$ Tregs. After the rats were euthanized, the spleen was isolated, and a single-cell suspension was prepared using Ficoll-Histopaque (Beijing Solarbio Science & Technology Co., Ltd.) density gradient centrifugation at 700 x g for 30 min at RT. Samples collected by centrifugation were treated with RPMI-1640 medium (cat. no. 11875093; Gibco; Thermo Fisher Scientific, Inc.) with 10% FBS (cat. no. c0235; Gibco; Thermo Fisher Scientific, Inc.) and 1% penicillin-streptomycin, and were re-suspended and counted at $1x10^7$ cells/ml. $CD4^+$ T cells and $CD4^+$ $CD25^+$ cells were sorted using the BD FACSAria™ III Cell Sorter (BD Biosciences). The sorted cells were centrifuged at 450 x g for 5 min at RT, counted at $1x10^6$ cells/100 μl per tube, then treated with 5 μl 2% BSA (cat. no. A8020; Beijing Solarbio Science & Technology Co., Ltd.) and incubated at RT in the dark for 10 min to block non-specific staining. This was followed by staining with fluorochrome-conjugated antibodies against surface markers FITC anti-rat CD4 (0.5 mg/ml; cat. no. 201505; BioLegend, Inc.) and PE anti-rat CD25 (0.2 mg/ml, cat. no. 202105; BioLegend, Inc.), and incubated in the dark at 4˚C for 30 min. The sorting procedure was repeated three times to assess the purity of the sorted cells, which was determined to be 95% by flow cytometry.

Cell Counting Kit-8 (CCK-8) assay. A total of $1x10^5$ of the sorted $CD4^+$ T cells and $CD4^+$ $CD25^+$ Tregs were cultured and resuspended in 100 μl culture medium (RPMI 1640 supplemented with 10% FCS, 1% L-glutamine, HEPES 1 M and 1% penicillin-streptomycin) in sterile plastic 96-well, flat-bottom

Table III. Sequences of synthesized oligonucleotides and primers used in the present study.

A, miRNA mimics and inhibitors	
Gene/oligonucleotide	Sequence (5'-3')
Rno-mimics NC	
Sense	UUCUCCGAACGUGUCACGUTT
Antisense	ACGUGACACGUUCGGAGAATT
Rno-miR-155-5p mimics	
Sense	UUAAUGCUAAUUGUGAUAGGGGU
Antisense	CCCUAUCACGAUUAGCAUUAAUU
Rno-miR-155-5p inhibitor NC	CAGUACUUUUGUGUAGUACAA
Rno-miR-155-5p inhibitor	ACCCCUAUCACAAUUAGCAUUAA
hsa-mimics NC	
Sense	UUGUGAAGGCAUAAUGGUGUCAUU
Antisense	AAUGACACCAUUAUGCCUUCACAA
hsa-miR-155-5p mimics	
Sense	UUAAUGCUAAUCGUGAUAGGGGUU
Antisense	AACCCCUAUCACGAUUAGCAUUAA
hsa-miR-155-5p inhibitor NC	CAGUACUUUUGUGUAGUACAA
hsa-miR-155-5p inhibitor	AACCCCTATCACGATTAGCATTAA

B, siRNAs	
Gene/oligonucleotide	Sequence (5'-3')
si-BCL10-1	
Sense	CCAAUUCUGAUGAGAGCAATT
Antisense	UUGCUCUCAUCAGAAUUGGTT
si-BCL10-2	
Sense	GGAAGUUGUUAGACUACUUTT
Antisense	AAGUAGUCUAACAACUUCCTT
si-BCL10-3	
Sense	GCUAAAGCUUCGGAAUAUATT
Antisense	UAUAUUCCGAAGCUUUAGCTT
si-NC	
Sense	UUCUCCGAACGUGUCACGUTT
Antisense	ACGUGACACGUUCGGAGAATT

C, Primers	
Gene/oligonucleotide	Sequence (5'-3')
Rno-miR-155-5p	
Forward	CTCCTACCTGTTAGCATTAACAAAA
Reverse	All-in-One™ miRNA RT-qPCR detection kit (GeneCopoeia, Inc.)
Rno-U6	Cat. no. RmiRQP9003 (GeneCopoeia, Inc.)
hsa-miR-155-5p	
Forward	GCTCCTACATATTAGCATTAACAAAAA
Reverse	All-in-One™ miRNA RT-qPCR detection kit (GeneCopoeia, Inc.)
hsa-U6	Cat. no. HmiRQP9001 (GeneCopoeia, Inc.)
BCL10	
Forward	ACCATCCAGAGGGAGAGTCG
Reverse	CTGTTTTCCAGCCTGCCAAC

Table III. Continued.

C, Primers	
Gene/oligonucleotide	Sequence (5'-3')
β-actin	
Forward	CCCGCGAGTACAACCTTCTT
Reverse	AACACAGCCTGGATGGCTAC
Foxp3	
Forward	TGGGATCAATGTGGCCAGTC
Reverse	GGTTGCTGTCTTTCCTGGGT
TGF-β1	
Forward	ACGTCAGACATTCGGGAAGC
Reverse	CGTGTTGCTCCACAGTTGAC
CTLA-4	
Forward	TGTACCCACCGCCATACTTTG
Reverse	CGAACTAACTGCAGCAAGGA
ICOS	
Forward	TCCTGCACTTCTTCCTGAAACA
Reverse	CTGTGACCTCAAAGGACCCTAC

NC, negative control; miRNA/miR, microRNA; BCL10, B-cell lymphoma/leukemia 10; si, siRNA; Foxp3, fork-head box protein 3; TGF-β1, transforming growth factor β1; CTLA-4, cytotoxic T-lymphocyte-associated protein 4; ICOS, inducible T cell costimulator; Rno, *Rattus norvegicus*; Hsa, *Homo sapiens*.

microwell culture plates (Thermo Fisher Scientific, Inc.) at 37˚C with 5% CO_2. For proliferation analysis, $CD4^+$ $CD25^+$ Tregs and $CD4^+$ T cells were cultured separately, and 100 μl control medium with or without phytohaemagglutinin (PHA) (cat. no. P8090; Beijing Solarbio Science & Technology Co., Ltd.) was added to the appropriate wells. The final concentration of PHA was 20 μg/ml. For suppression analysis, $CD4^+$ T cells and $CD4^+$ $CD25^+$ Tregs were co-cultured at a 1:1 ratio ($0.5x10^5$ + $0.5x10^5$) for 96 h in the same conditions. Tregs inhibitory capacity was assessed using CCK-8 assay (Beyotime Institute of Biotechnology). A 10 μl solution of CCK-8 reagent was added to the cells and incubated with 5% CO_2 at 37˚C for 2 h. The absorbance of samples was then measured at 450 nm using a Multiskan™ FC microplate reader.

Verification of the function of BCL10 in Tregs. To explore the function of BCL10 in Tregs, $CD4^+$ $CD25^+$ Tregs were transfected with 20 μM BCL10 small interfering (si)RNA, scramble siRNA (si-NC; Table III; Shanghai GenePharma Co., Ltd.), 20 μM miR-155-5p inhibitor or inhibitor NC (Table III; Shanghai GenePharma Co., Ltd.) in 24-well plates with $1x10^6$ cells/well using Entranster™-R4000 according to the manufacturer's instructions. After incubation with 5% CO_2 at 37˚C for 4 h, the cells were placed in fresh RPMI-1640 medium with 10% FCS, 1% L-glutamine, 1% sodium pyruvate, 1% non-essential amino acids, $2x10^{-5}$ M 2-mercaptoethanol and 1% penicillin-streptomycin, followed by stimulation with 5 μg/ml anti-CD3 (cat. no. 201415; BioLegend, Inc.) and 5 μg/ml anti-CD28 (cat. no. 200902; BioLegend, Inc.) monoclonal antibodies in the presence of IL-2 (100 U/ml; PeproTech, Inc.) at 37˚C for 48 h. To evaluate the activation of Tregs, the TGF-β1 and IL-10 levels in the cell supernatant were measured using an ELISA kit (cat. no. ml002856; cat. no. ERC004; Neobioscience Technology Co., Ltd.) according to the manufacturer's instructions.

Western blotting. $CD4^+$ $CD25^+$ Treg cells were lysed with RIPA buffer (cat. no. 89901; Thermo Fisher Scientific, Inc.) and the protein concentration was quantified using the BCA method. A total of 150 μg proteins from each sample were separated by SDS-PAGE using a 5% concentration and a 15% separation gel and then transferred to a 0.22 μm polyvinylidene fluoride membrane. Next, the membranes were blocked in 5% non-fat dried milk (cat. no. D8340; Beijing Solarbio Science & Technology Co., Ltd.) in Tris-buffered saline containing 0.05% Tween 20 (TBST) [0.05% (v/v) Tween 20 in 20 mmol/l Tris-HCl buffer, pH 7.6, containing 137 mm sodium chloride] for 1 h at RT. The membranes were incubated with primary antibodies including mouse anti-BCL10 (1:1,000; cat. no. BM1565; Wuhan Boster Biological Technology, Ltd.) and mouse anti-β-actin (1:1,000; cat. no. 3700; Cell Signaling Technology, Inc.) overnight at 4˚C. The membranes were washed three times with TBST, and incubated with HRP-labeled goat anti-mouse secondary IgG antibody (zb-2305; OriGene Technologies, Inc.) for 2 h at RT. Protein bands were visualized with Immobilon Western Chemiluminescent HRP Substrate (Millipore, USA) and captured by MiniChemi 610 Plus imaging system (Beijing Sage Creation Science Co., Ltd.). Bands were quantified using ImageJ (Ver. 1.46; National Institutes of Health) and normalized to β-actin.

RT-qPCR. Initially, fresh whole blood was diluted in 1% PBS at a ratio of 1:3 and then centrifuged at 450 x g for 10 min at RT to eliminate red cells in 10 ml of red blood cell lysis buffer (C3702; Beyotime Institute of Biotechnology). Subsequently, peripheral blood mononuclear cells (PBMC) were isolated through Ficoll density gradient centrifugation at 700 x g for 30 min at RT. Total RNA was then extracted from either PBMC or Tregs using TRIzol® reagent (Invitrogen; Thermo Fisher Scientific, Inc.) in accordance with the manufacturer's guidelines, and subsequently reverse transcribed into complementary DNA (cDNA) using a PrimeScript™ RT reagent Kit (Takara Biotechnology Co., Ltd.) as per the manufacturer's instructions. The relative expression levels of miR-155-5p were quantified using the All-in-One™ miRNA RT-qPCR detection kit (GeneCopoeia, Inc.). The primer sequences used in the present study are presented in Table III, and were purchased from GeneCopoeia, Inc. The reverse primers were included in the All-in-One™ miRNA RT-qPCR detection kit. The thermocycling conditions used were as follows: Initial denaturation for 30 sec at 95˚C; followed by 40 cycles of 5 sec at 95˚C, 30 sec at 60˚C and 30 sec at 72˚C. mRNAs for BCL10, TGF-β1, Foxp3, cytotoxic T-lymphocyte-associated protein 4 (CTLA-4) and inducible T-cell costimulator (ICOS) were reverse transcribed using the RevertAid First Strand cDNA Synthesis Kit (Thermo Fisher Scientific, Inc.), and qPCR was performed using SYBR Green Real-time PCR Master Mix (Thermo Fisher Scientific, Inc.). The thermocycling conditions used were as follows: Uracil-DNA glycosylase enzyme activation for 2 min at 50˚C and predenaturation for 2 min at 95˚C, followed by 40 cycles of 15 sec at 95˚C and 1 min at 60˚C. The $2^{-\Delta\Delta Cq}$ method (32) was used for the calculation of relative expression levels normalized to β-actin (for mRNA) or U6 (for miRNA). Data analysis was performed using CFX 96 software (Bio-Rad Laboratories, Inc.).

Statistical analysis. All experiments were performed in three independent biological replicates unless stated otherwise, and the data are presented as the mean ± standard error of the mean or the median (interquartile range). Data were analyzed using GraphPad Prism (version 9.1; GraphPad Software; Dotmatics). Correlations were analyzed using Pearson's correlation test. The means of the two groups were compared using an unpaired Student's t-test, while the Mann-Whitney U test was utilized for Lennon's score. One-way analysis of variance followed by Tukey's post hoc test was used for comparisons among multiple groups. Additionally, two-way ANOVA followed by Bonferroni's post hoc test was employed to analyze the CCK-8 data. Fisher's exact test was used to compare the sex distribution between the MG group and non-MG groups, which is presented as n (%). P<0.05 was considered to indicate a statistically significant difference.

Results

miR-155-5p expression level is associated with the QMG score and BCL10 mRNA expression level in patients with MG. RT-qPCR results demonstrated that the expression level of miR-155-5p was significantly higher in PBMCs from patients with MG compared with that of the control group (Fig. 1A).

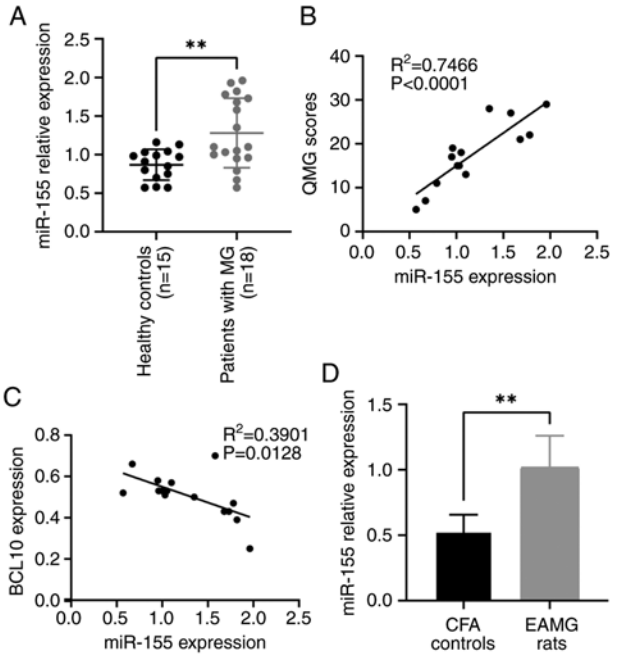

Figure 1. Expression levels of miR-155-5p in MG and its association with QMG score and BCL10 mRNA levels. (A) Expression levels of miR-155-5p in patients with MG were significantly higher compared with those in the control group. (B) QMG scores of patients with MG positively correlated with the expression levels of miR-155-5p (R^2=0.7466; P<0.0001). (C) Expression levels of BCL10 mRNA negatively correlated with those of miR-155-5p in patients with MG (R^2=0.3901; P=0.0128). (D) Expression levels of miR-155-5p in EAMG rats were significantly higher compared with those in the control group. Data are presented as the mean ± standard error of the mean. **P<0.01. MG, myasthenia gravis; QMG, quantitative MG; EAMG, experimental autoimmune myasthenia gravis; CFA, complete Freund's adjuvant; miR, microRNA; BCL10, B-cell lymphoma/leukemia 10.

Furthermore, there was a significant positive correlation between the expression levels of miR-155-5p and QMG scores (R^2=0.7466; Fig. 1B). A significant negative correlation was observed between the expression levels of miR-155-5p and the levels of BCL10 mRNA in the blood (R^2=0.3901; Fig. 1C). Furthermore, the expression level of miR-155-5p in rats with EAMG was significantly higher compared with that in control rats (Fig. 1D).

Clinical manifestation, weight evolution and Lennon score of rats with EAMG. The rats in the EAMG group demonstrated weakness, weight loss, dull coats and listlessness in the 11 days following R97-116 peptide immunization, and an inflammatory response characterized by redness, swelling and pain was observed at the injection sites (data not shown). In addition, hypoactivity was observed, including reduced crawling and grip, weak bite and vocalization and reduced food intake in rats with EAMG. At 45 days following immunization, the body weight of rats with EAMG (186.7±0.63 g) was significantly lower compared with that of the control group (211.7±0.64 g) (Fig. 2A). The Lennon scores of the EAMG group 1.63 (0.31) [median (interquartile range)] were significantly higher compared with those of the control group 0.50 (0.3) (Fig. 2B). The ELISA results demonstrated that the level of serum anti-AChR antibodies in the EAMG group (453.70±16.23) was significantly higher compared with that of the control group (222.30±19.75) (Fig. 2C). These results

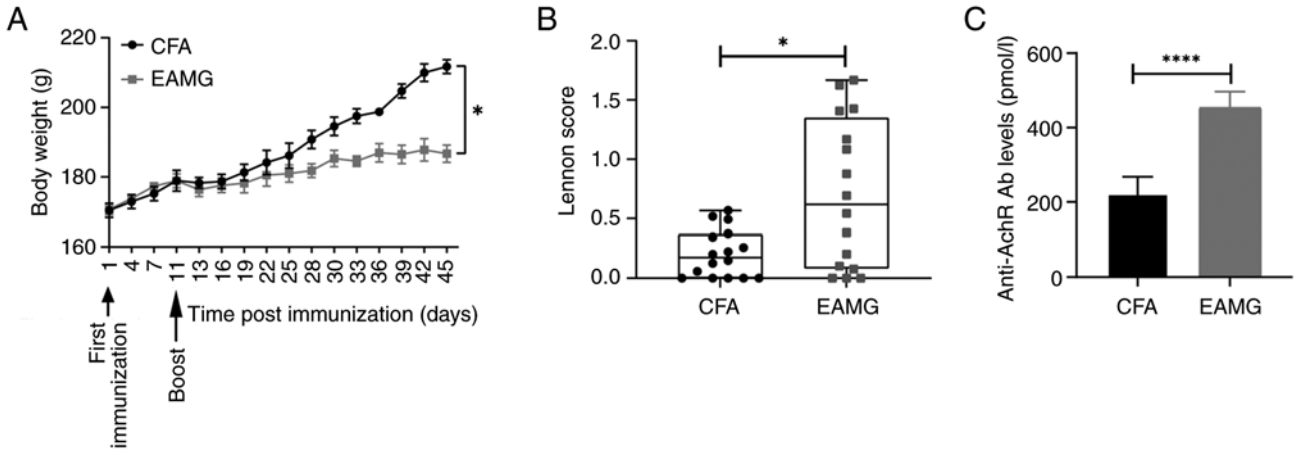

Figure 2. Establishment of the rat model of EAMG. (A) Body weight of rats with EAMG was significantly decreased compared with that of the CFA group. (B) Lennon scores were significantly increased in rats with EAMG compared with the CFA group. (C) Levels of serum anti-AchR Ab were significantly increased in rats with EAMG at 45 days compared with those in the CFA group. Data are presented as the mean ± standard error of the mean. *P<0.05 and ****P<0.0001. EAMG, experimental autoimmune myasthenia gravis; CFA, complete Freund's adjuvant; AchR Ab, acetylcholine receptor antibody.

indicated the successful establishment of the rat model of EAMG.

BCL10 is a direct target of miR-155-5p. The TargetScan 8.0 software search indicated that BCL10 was a potential target of miR-155-5p, as demonstrated by the complementary sequences between BCL10 3'-UTR and miR-155-5p (Fig. 3A and B). miR-155-5p mimics or mimics NC were introduced via transfection into 293T cells. Similarly, miR-155-5p mimics or mimics NC, along with miR-155-5p inhibitor or inhibitor NC, were transfected into Jurkat T cells. The expression levels of miR-155-5p were quantitatively assessed using RT-qPCR in 293T and Jurkat cells, demonstrating the success of the transfections (Fig. 3C, E and F). Luciferase assay results demonstrated that co-transfection with miR-155-5p mimics led to a significant ~55% decrease in the luciferase activity of BCL10-WT-transfected cells compared with the mimics NC group, indicating that BCL10 specifically binds to miR-155-5p. However, no significant change was observed in BCL10-Mut-transfected cells (Fig. 3D). Moreover, the study revealed that transfection of miR-155-5p mimics resulted in a significant decrease in mRNA and a notable downregulation of protein expression levels of BCL10 in Jurkat T cells, as compared to the transfection of mimics NC. Conversely, transfection of miR-155-5p inhibitor led to a significant increase in mRNA and a marked upregulation of protein expression levels of BCL10 in Jurkat T cells, as compared to the transfection of inhibitor NC (Fig. 3G and H). These results demonstrated that BCL10 is a direct target of miR-155-5p.

Proportion of Tregs is significantly decreased in patients with MG and rats with EAMG. FACS analysis revealed that the proportion of circulating Tregs was significantly decreased in patients with MG compared with that in the control group (3.70±0.41% vs. 5.77±0.59%, respectively; Fig. 4A and C). The proportion of Tregs was also significantly decreased in the spleen of rats with EAMG compared with that in the CFA group (0.47±0.04% vs. 0.80±0.04%, respectively; Fig. 4B and D).

BCL10 is related to the activation and suppressive function of Tregs. To clarify the biological functions of BCL10 in $CD4^+$ $CD25^+$ Tregs, BCL10 expression was knocked down using siRNA. si-NC and si-BCL10-1, -2 and -3 were transfected into cells and BCL10 expression levels were measured using RT-qPCR and western blotting (Fig. 5A and B). si-BCL10-1 was the most efficient siRNA in significantly reducing the expression of BCL10 at both the mRNA and protein levels compared with the corresponding control groups, and was selected for use in subsequent experiments. Additionally, the expression levels of miR-155-5p were significantly decreased in $CD4^+$ $CD25^+$ Tregs after transfection with miR-155-5p inhibitor compared with those in the control group, as demonstrated by RT-qPCR (Fig. 5C). These results indicated that the aforementioned transfections were successful. In addition, miR-155-5p inhibitor transfection notably increased the mRNA and protein expression levels of BCL10 (Fig. 5D and E). Both the levels of TGF-β1 and IL-10 in the cell supernatant were significantly reduced in the si-BCL10 group and elevated in the miR-155-5p inhibitor group, as compared to their respective control groups. These findings suggest that BCL10 plays a role in the activation of Tregs (Fig. 5F and G). The CCK-8 assay was employed to assess the suppressive capacity of $CD4^+$ $CD25^+$ Tregs on the proliferation of $CD4^+$ T cells. The results demonstrated that $CD4^+$ T-cell proliferation in both the inhibitor NC group and the si-BCL10 group exhibited a significant increase after 72 h of $CD4^+$ T cells and $CD4^+$ $CD25^+$ Tregs were co-culture compared with the miR-155-5p inhibitor group. Furthermore, after 96 h of $CD4^+$ T cell and $CD4^+$/$CD25^+$ Treg co-culture, the proliferation of $CD4^+$ T cells in the si-BCL10 group was significantly higher compared with that in the si-NC group. Additionally, the proliferation of $CD4^+$ T cells in both the inhibitor NC group and the si-BCL10 group was significantly increased compared with that in the miR-155-5p inhibitor group. These findings suggest that BCL10 knockdown resulted in a decrease in the suppressive capacity of Tregs on $CD4^+$ T cell proliferation, while the inhibition of miR-155-5p expression weakened the inhibition

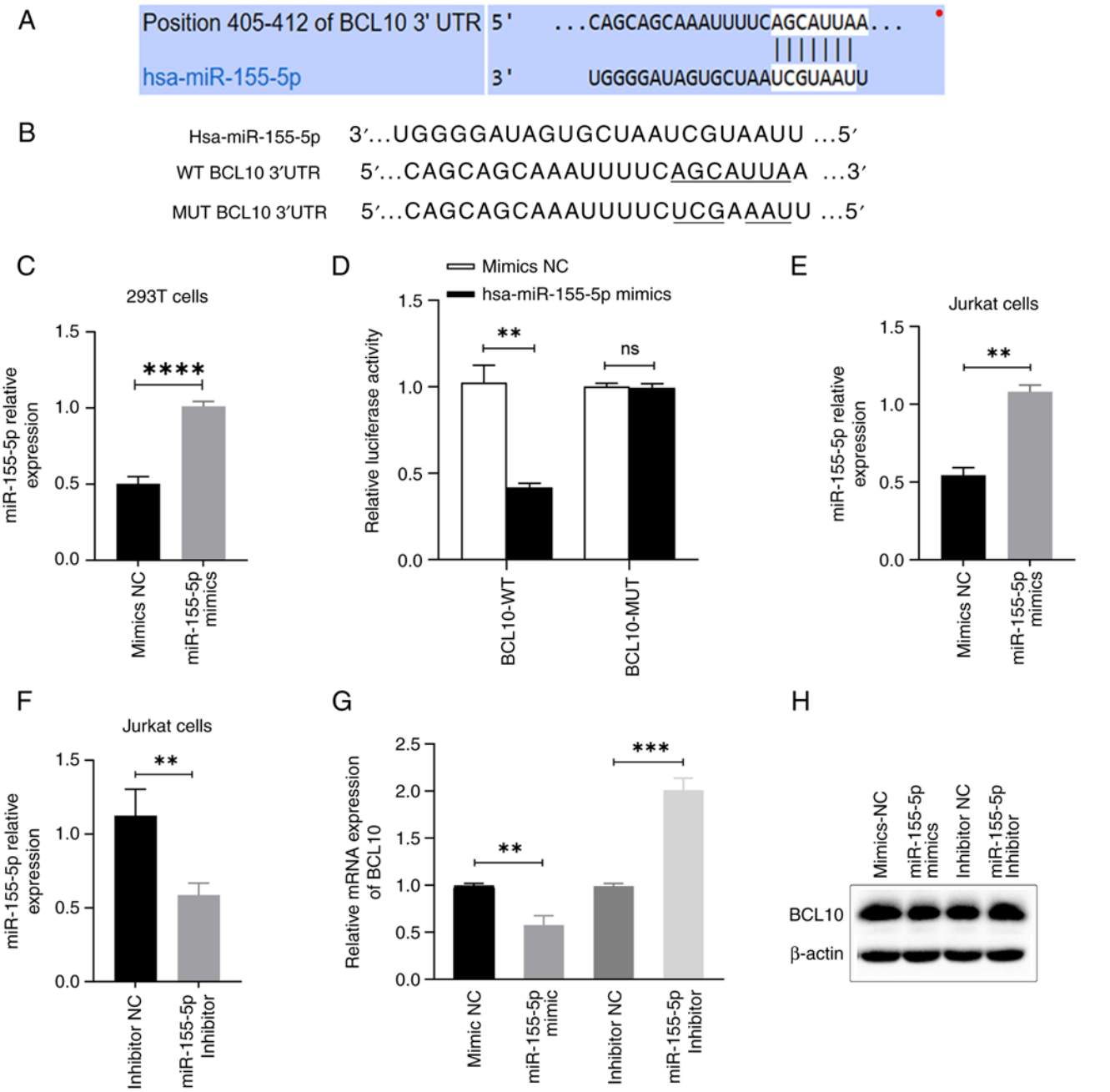

Figure 3. BCL10 is a direct target of miR-155-5p. (A) TargetScan predicted the binding sites of miR-155-5p in the 3'-UTR of BCL10. (B) miR-155-5p, WT BCL10 3'-UTR and Mut BCL10 3'-UTR sequences. (C) Relative expression levels of miR-155-5p assessed in 293T cells transfected with miR-155-5p mimics and mimics NC. (D) Luciferase activity of WT and Mut BCL10 3'-UTR reporter genes in the presence or absence of miR-155-5p. (E) Relative expression of miR-155-5p in Jurkat cells transfected with miR-155-5p mimics. (F) Relative expression of miR-155-5p in Jurkat cells transfected with miR-155-5p inhibitor. (G) mRNA expression levels of BCL10 following transfection with miR-155-5p mimics and inhibitor. (H) Representative western blot assay depicting the protein levels of BCL10 following transfection with miR-155-5p mimics and inhibitor. **P<0.01, ***P<0.001 and ****P<0.0001. Data are presented as the mean ± standard error of the mean. ns, not significant; BCL10, B-cell lymphoma/leukemia 10; NC, negative control; UTR, untranslated region; MUT, mutant; WT, wild-type; miR, microRNA.

of the BCL10 gene, potentially exhibiting an indirect impact on the suppressive ability of Tregs on $CD4^+$ T cell proliferation (Fig. 5H). Furthermore, the expression levels of Foxp3, TGF-β1, CTLA-4 and ICOS were significantly decreased in Tregs transfected with si-BCL10 and significantly increased in Tregs transfected with miR-155-5p inhibitor compared with those in the corresponding controls (Fig. 5I-L). These results indicated that BCL10 affects the activation of Tregs and their immunosuppressive functions.

Discussion

The current study revealed an upregulation of miR-155-5p expression in both patients diagnosed with MG and rats with EAMG when compared to their respective control groups. Through use of a dual-luciferase reporter assay, it was established that BCL10 is a direct target of miR-155-5p. Furthermore, this study presented evidence supporting a connection between miR-155-5p/BCL10 signaling and compromised Treg function.

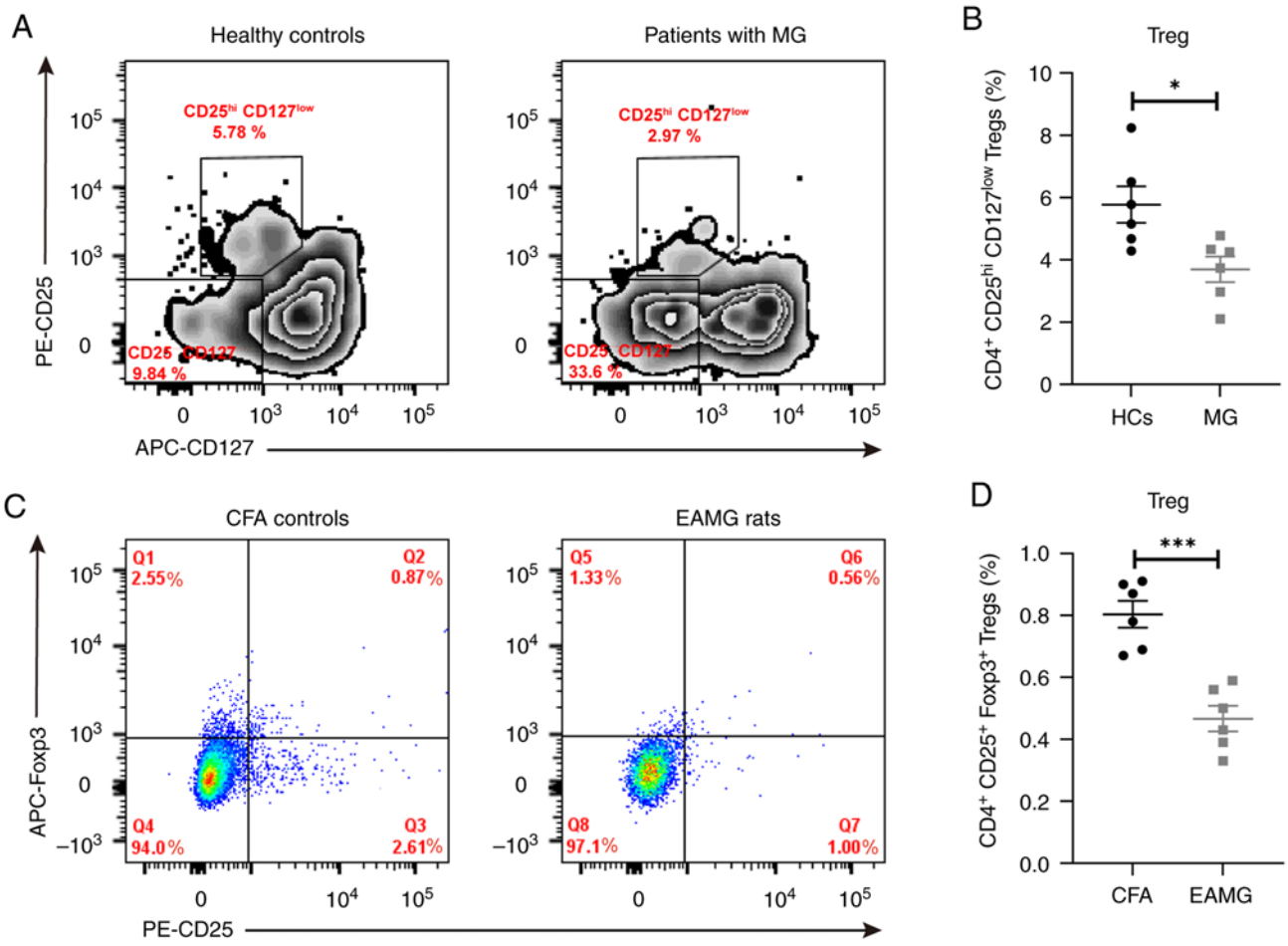

Figure 4. Proportion of Tregs in patients with MG and rats with EAMG. (A) Flow cytometry pseudocolor analysis of $CD4^+$ $CD25^{hi}$ $CD127^{low}$ Tregs in patients with MG and HCs. (B) Proportion of peripheral blood Tregs in $CD4^+$ Tregs of patients with MG and HCs. (C) Flow cytometry dot plot analysis of $CD4^+CD25^+$ $Foxp3^+$ Tregs in rats with EAMG and the CFA group. (D) Proportion of $CD4^+$ Tregs in the spleens of rats with EAMG and the CFA group. Data are presented as the mean ± standard error of the mean. $^*P<0.05$ and $^{***}P<0.001$. MG, myasthenia gravis; EAMG, experimental autoimmune myasthenia gravis; CFA, complete Freund's adjuvant; Treg, regulatory T cell; PE, phycoerythrin; APC; allophycocyanin; Foxp3, fork-head box protein 3; HCs, healthy controls.

miRNAs have previously been reported to participate in certain physiological processes, including immune regulation and homeostasis (33-36). A previous study reported that miR-142-3p targets Tet methylcytosine dioxygenase 2 and impairs the differentiation of Tregs and their stability in type 1 diabetes (37). Another previous study demonstrated that miR-34a targets Foxp3, an essential regulator of Treg development and function (38). Furthermore, Kim *et al* (39) predicted that miR-342-3p could directly target components of mTOR complex 2, which inhibits the development of Tregs (40). Foxp3 has previously been reported to bind to an intron region of the gene that encodes the mRNA precursor of miR-155-5p, and is associated with the regulation of activation and immunosuppressive function of Tregs (41,42). As immune activation and the disruption of immune homeostasis are tightly associated with the pathogenesis of MG, and the expression of miRNAs can be specifically inhibited or mimicked, miRNAs that regulate the function of Tregs may be promising targets for the management of MG.

The precise impact of miRNAs on immune regulation and the involvement of miRNAs and their target genes in the pathogenesis of MG has been previously investigated, indicating that miRNA plays an important role in the development of MG (43). In the present study, it was found that the expression level of miR-155-5p was significantly increased in patients with MG, which is consistent with the results of a previous study by Wang *et al* (20). The QMG score can be used to evaluate the severity of MG and response to treatment (25,26). The present study demonstrated that the expression level of miR-155-5p was positively correlated with the QMG score, and thus, the severity of MG. Meanwhile, an increased expression level of miR-155-5p was observed in EAMG rats compared with the control group. These results suggest that miR-155-5p is closely related to the pathogenesis of MG.

BCL10 is member of the lymphoid caspase recruitment domain (CARD) 11-BCL10-mucosa-associated lymphoid tissue lymphoma 1 (MALT1) and myeloid-CARD9-BCL10-MALT1 tripartite complexes that transduce signals from immunoreceptor tyrosine-based activation motif-coupled receptors in lymphoid and myeloid immune cells (44). Yang *et al* (22) reported that BCL10 is necessary for the development and suppressive function of $Foxp3^+$ Tregs, the proportion of effector Tregs and the expression of a series of Treg-cell effector and suppressive genes were significantly decreased in BCL10-deficient Tregs. Rosenbaum *et al* (21) reported that

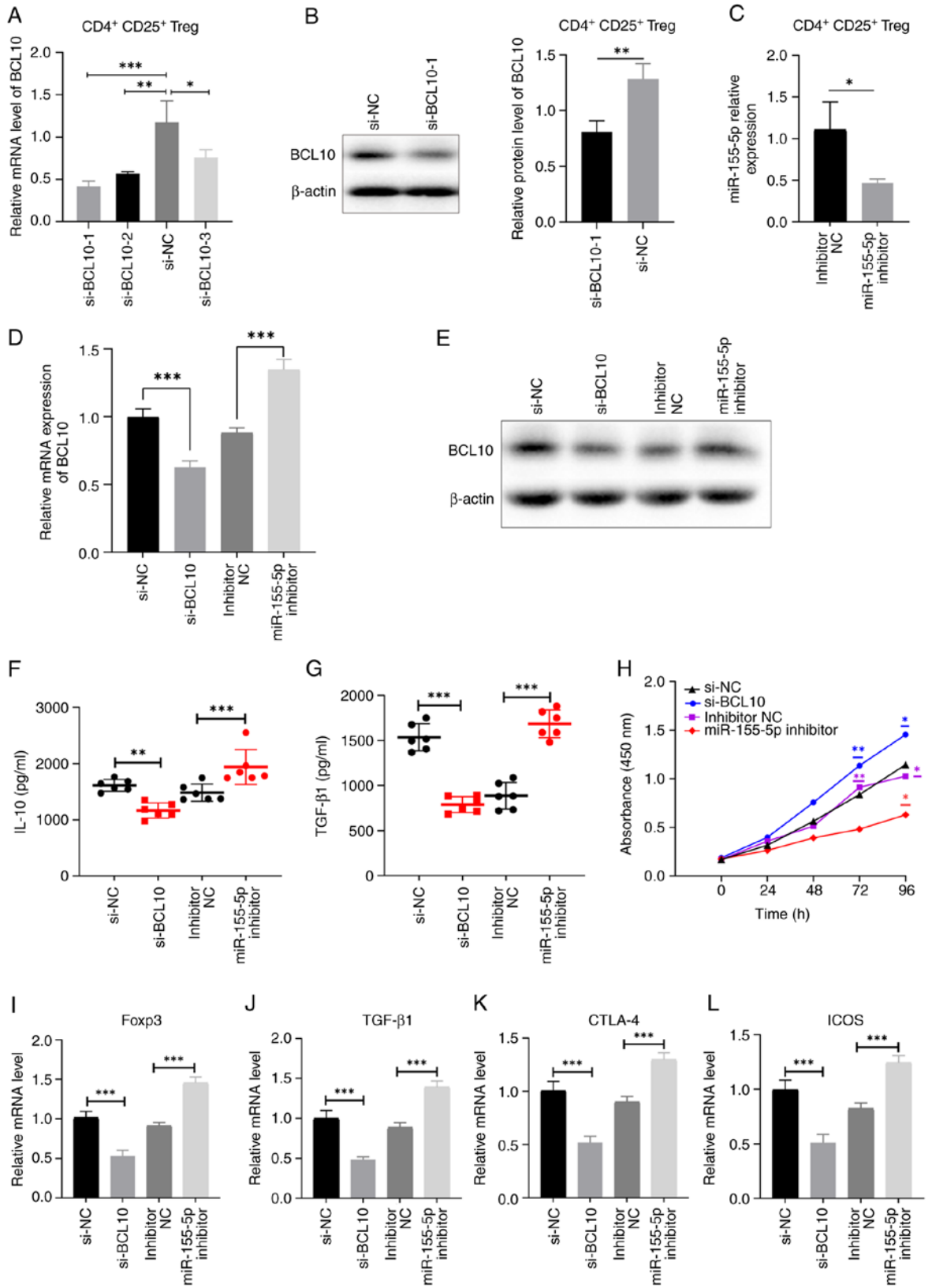

Figure 5. BCL10 mediates Treg activation and immunosuppressive functions. (A) Reverse transcription-quantitative PCR and (B) western blotting was used to measure the expression levels of BCL10 in cells transfected with siRNAs targeting BCL10. (C) Relative expression levels of miR-155-5p in $CD4^+$ $CD25^+$ Tregs transfected with miR-155-5p inhibitor and inhibitor NC. BCL10 (D) mRNA and (E) protein expression levels decreased in cells transfected with si-BCL10 and increased in the miR-155-inhibitor group compared with controls. Serum levels of (F) IL-10 and (G) TGF-β1 significantly decreased in the si-BCL10 group and increased in the miR-155-inhibitor group, compared with controls. (H) Cell Counting Kit-8 assay demonstrated that $CD4^+$ T cell proliferation significantly increased at 96 h following BCL10 knockdown, while significantly decreased with miR-155-5p inhibition, compared with the respective control groups. mRNA expression levels of (I) Foxp3, (J) TGF-β1, (K) CTLA-4 and (L) ICOS in cells transfected with si-BCL10, miR-155-5p inhibitor and respective transfection controls. Data are presented as the mean ± standard error of the mean. *P<0.05, **P<0.01 and ***P<0.001. BCL10, B-cell lymphoma/leukemia 10; Treg, regulatory T cell, NC, negative control; Foxp3, fork-head box protein 3; TGF-β1, transforming growth factor β1; CTLA-4, cytotoxic T-lymphocyte-associated protein 4; ICOS, inducible T cell costimulator; si, siRNA; miR, microRNA.

BCL10-deficient effector Tregs cannot express CTLA-4, OX40, programmed cell death protein 1 or T cell immunoreceptor with Ig and ITIM domains, which are cooperatively involved in Treg-mediated immune suppression. In the present study, the binding of miR-155-5p and BCL10 was further confirmed by bioinformatics analysis and a dual-luciferase reporter assay. Inhibition of miR-155-5p *in vitro* resulted in increased mRNA and protein expression levels of BCL10, further supporting the notion of BCL10 as a direct target of miR-155-5p.

Treg dysfunction is associated with a number of autoimmune diseases, such as systemic lupus erythematosus and rheumatoid arthritis (45). The present study demonstrated that the proportion of $CD4^+$ $CD25^{hi}$ $CD127^{low}$ Tregs significantly decreased in the peripheral blood of patients with MG and the spleens of rats with EAMG compared with the respective controls, which suggested that the proportion of Tregs is dysregulated in MG. Furthermore, BCL10 knockdown significantly inhibited, while miR-155-5p inhibitor significantly increased the activation and immunosuppressive function of $CD4^+$ $CD25^+$ Tregs compared with controls. It was found that the impaired immunosuppressive function of Tregs was associated with the levels of BCL10 and miR-155-5p, and miR-155-5p may regulate Treg cell activation by directly targeting BCL10.

There are certain limitations to the present study. These include the utilization of diverse sample sources and distinct Foxp3 markers for the detection of Tregs in patients with MG and the rat model of EAMG. Consequently, significant variations in the proportion of Tregs between patients and the animal model were observed. This discrepancy may also be attributed to the disparate cellular origins of the human and rat samples utilized in the flow cytometry analysis, along with the divergent selection of cell markers for gating. Furthermore, existing literature also suggests that the percentage of Tregs in the peripheral blood of patients with MG surpass those in the spleen of EAMG animal models (46-49). Another limitation of the present study was that the demographic information of patients with MG and healthy controls was not strictly matched, as well as the failure to eliminate confounding factors such as the duration of disease in patients with MG and the unrestricted influence of drug treatment, which may influence the validity of the clinical findings. Furthermore, the differential expression levels of miR-155-5p and BCL10 in patients with MG and rats with EAMG were not confirmed by gene sequencing; therefore, future studies are required to further investigate the underlying mechanisms of the miR-155-5p/BCL10 axis on the development of MG.

In conclusion, the present study demonstrated that the expression levels of BCL10 in patients with MG significantly negatively correlated with the expression levels of miR-155-5p, which suggests that miR-155-5p is involved in the pathogenesis of MG and is associated with BCL10. Furthermore, Treg activation and functional changes in the presence of BCL10 siRNA provided additional support for the functional relevance and homeostasis of the miR-155-5p/BCL10 axis in the regulation of Tregs in MG. In conclusion, the present study demonstrated that miR-155-5p inhibited the activation and immunosuppressive function of Tregs potentially by targeting BCL10, which may constitute a future possible target for the treatment of MG.

Acknowledgements

Not applicable.

Funding

This study was supported by the Talent Innovation and Entrepreneurship Project of Lanzhou City, Gansu Province (grant no. 2020-RC-47), the Cuiying Scientific and Technological Innovation Program in Lanzhou University Second Hospital (grant no. CY2021-QN-A08), the 2022 Provincial Key Talent Project-Neural Infection and Immune Diseases Precision Diagnosis and Treatment Network Platform Construction (grant no. 2022-77-6) and the Lanzhou Science and Technology Program Project (grant no. 2021-1-177).

Availability of data and materials

The datasets used and/or analyzed during the current study are available from the corresponding author on reasonable request.

Authors' contributions

JS and MS designed the study. QX and WZ performed the bioinformatics analysis. JS and QX conducted the experiments. MW and XL confirm the authenticity of all the raw data. JS, XL and MW performed the statistical analyses and the interpretation of data. JS and MS wrote the manuscript. QX and XL provided valuable opinions in the process of writing the manuscript. XL and MW revised the manuscript. All authors read and approved the final version of the manuscript.

Ethics approval and consent to participate

The study involving human participants was reviewed and approved by the Lanzhou University Second Hospital Ethics Committee (approval no. 2021A-445; Lanzhou, China). The patients/participants provided written informed consent to participate in the present study. The Institutional Animal Care and Use Committee of Lanzhou University Second Hospital approved the animal experimental protocol (approval no. 2021A-319; Lanzhou, China).

Patient consent for publication

Not applicable.

Competing interests

The authors declare that they have no competing interests.

References

1. Gilhus NE, Tzartos S, Evoli A, Palace J, Burns TM and Verschuuren JJGM: Myasthenia gravis. Nat Rev Dis Primers 5: 30, 2019.
2. Dresser L, Wlodarski R, Rezania K and Soliven B: Myasthenia gravis: Epidemiology, pathophysiology and clinical manifestations. J Clin Med 10: 2235, 2021.
3. Danikowski KM, Jayaraman S and Prabhakar BS: Regulatory T cells in multiple sclerosis and myasthenia gravis. J Neuroinflammation 14: 117, 2017.

4. Cron MA, Guillochon É, Kusner L and Le Panse R: Role of miRNAs in normal and myasthenia gravis thymus. Front Immunol 11: 1074, 2020.
5. Villegas JA, Van Wassenhove J, Le Panse R, Berrih-Aknin S and Dragin N: An imbalance between regulatory T cells and T helper 17 cells in acetylcholine receptor-positive myasthenia gravis patients. Ann N Y Acad Sci 1413: 154-162, 2018.
6. Balandina A, Lécart S, Dartevelle P, Saoudi A and Berrih-Aknin S: Functional defect of regulatory CD4(+)CD25+ T cells in the thymus of patients with autoimmune myasthenia gravis. Blood 105: 735-741, 2005.
7. Thiruppathi M, Rowin J, Ganesh B, Sheng JR, Prabhakar BS and Meriggioli MN: Impaired regulatory function in circulating CD4(+)CD25(high)CD127(low/-) T cells in patients with myasthenia gravis. Clin Immunol 145: 209-223, 2012.
8. Battaglia A, Di Schino C, Fattorossi A, Scambia G and Evoli A: Circulating CD4+CD25+ T regulatory and natural killer T cells in patients with myasthenia gravis: A flow cytometry study. J Biol Regul Homeost Agents 19: 54-62, 2005.
9. Fuchs S, Aricha R, Reuveni D and Souroujon MC: Experimental autoimmune myasthenia gravis (EAMG): From immunochemical characterization to therapeutic approaches. J Autoimmun 54: 51-59, 2014.
10. Gradolatto A, Nazzal D, Truffault F, Bismuth J, Fadel E, Foti M and Berrih-Aknin S: Both treg cells and tconv cells are defective in the myasthenia gravis thymus: Roles of IL-17 and TNF-α. J Autoimmun 52: 53-63, 2014.
11. Rodríguez-Perea AL, Arcia ED, Rueda CM and Velilla PA: Phenotypical characterization of regulatory T cells in humans and rodents. Clin Exp Immunol 185: 281-291, 2016.
12. Gavin MA, Rasmussen JP, Fontenot JD, Vasta V, Manganiello VC, Beavo JA and Rudensky AY: Foxp3-dependent programme of regulatory T-cell differentiation. Nature 445: 771-775, 2007.
13. Vrolix K, Fraussen J, Losen M, Stevens J, Lazaridis K, Molenaar PC, Somers V, Bracho MA, Le Panse R, Stinissen P, *et al*: Clonal heterogeneity of thymic B cells from early-onset myasthenia gravis patients with antibodies against the acetylcholine receptor. J Autoimmun 52: 101-112, 2014.
14. Serr I, Fürst RW, Ott VB, Scherm MG, Nikolaev A, Gökmen F, Kälin S, Zillmer S, Bunk M, Weigmann B, *et al*: miRNA92a targets KLF2 and the phosphatase PTEN signaling to promote human T follicular helper precursors in T1D islet autoimmunity. Proc Natl Acad Sci USA 113: E6659-E6668, 2016.
15. Serr I, Scherm MG, Zahm AM, Schug J, Flynn VK, Hippich M, Kälin S, Becker M, Achenbach P, Nikolaev A, *et al*: A miRNA181a/NFAT5 axis links impaired T cell tolerance induction with autoimmune type 1 diabetes. Sci Transl Med 10: eaag1782, 2018.
16. Zhou X, Jeker LT, Fife BT, Zhu S, Anderson MS, McManus MT and Bluestone JA: Selective miRNA disruption in T reg cells leads to uncontrolled autoimmunity. J Exp Med 205: 1983-1991, 2008.
17. O'Connell RM, Kahn D, Gibson WS, Round JL, Scholz RL, Chaudhuri AA, Kahn ME, Rao DS and Baltimore D: MicroRNA-155 promotes autoimmune inflammation by enhancing inflammatory T cell development. Immunity 33: 607-619, 2010.
18. Seddiki N, Brezar V, Ruffin N, Lévy Y and Swaminathan S: Role of miR-155 in the regulation of lymphocyte immune function and disease. Immunology 142: 32-38, 2014.
19. Ghafouri-Fard S, Azimi T, Hussen BM, Taheri M and Jalili Khoshnoud R: A review on the role of non-coding RNAs in the pathogenesis of myasthenia gravis. Int J Mol Sci 22: 12964, 2021.
20. Wang YZ, Tian FF, Yan M, Zhang JM, Liu Q, Lu JY, Zhou WB, Yang H and Li J: Delivery of an miR155 inhibitor by anti-CD20 single-chain antibody into B cells reduces the acetylcholine receptor-specific autoantibodies and ameliorates experimental autoimmune myasthenia gravis. Clin Exp Immunol 176: 207-221, 2014.
21. Rosenbaum M, Gewies A, Pechloff K, Heuser C, Engleitner T, Gehring T, Hartjes L, Krebs S, Krappmann D, Kriegsmann M, *et al*: Bcl10-controlled Malt1 paracaspase activity is key for the immune suppressive function of regulatory T cells. Nat Commun 10: 2352, 2019.
22. Yang D, Zhao X and Lin X: Bcl10 is required for the development and suppressive function of Foxp3$^+$ regulatory T cells. Cell Mol Immunol 18: 206-218, 2021.
23. Wei TT, Cheng Z, Hu ZD, Zhou L and Zhong RQ: Upregulated miR-155 inhibits inflammatory response induced by C. albicans in human monocytes derived dendritic cells via targeting p65 and BCL-10. Ann Transl Med 7: 758, 2019.
24. Berrih-Aknin S, Frenkian-Cuvelier M and Eymard B: Diagnostic and clinical classification of autoimmune myasthenia gravis. J Autoimmun 48-49: 143-148, 2014.
25. Jaretzki A III, Barohn RJ, Ernstoff RM, Kaminski HJ, Keesey JC, Penn AS and Sanders DB: Myasthenia gravis: Recommendations for clinical research standards. Task force of the medical scientific advisory board of the myasthenia gravis foundation of America. Neurology 55: 16-23, 2000.
26. Bedlack RS, Simel DL, Bosworth H, Samsa G, Tucker-Lipscomb B and Sanders DB: Quantitative myasthenia gravis score: Assessment of responsiveness and longitudinal validity. Neurology 64: 1968-1970, 2005.
27. Baggi F, Annoni A, Ubiali F, Milani M, Longhi R, Scaioli W, Cornelio F, Mantegazza R and Antozzi C: Breakdown of tolerance to a self-peptide of acetylcholine receptor alpha-subunit induces experimental myasthenia gravis in rats. J Immunol 172: 2697-2703, 2004.
28. Laferriere CA and Pang DS: Review of intraperitoneal injection of sodium pentobarbital as a method of euthanasia in laboratory rodents. J Am Assoc Lab Anim Sci 59: 254-263, 2020.
29. Losen M, Martinez-Martinez P, Molenaar PC, Lazaridis K, Tzartos S, Brenner T, Duan RS, Luo J, Lindstrom J and Kusner L: Standardization of the experimental autoimmune myasthenia gravis (EAMG) model by immunization of rats with Torpedo californica acetylcholine receptors-recommendations for methods and experimental designs. Exp Neurol 270: 18-28, 2015.
30. Cossarizza A, Chang HD, Radbruch A, Acs A, Adam D, Adam-Klages S, Agace WW, Aghaeepour N, Akdis M, Allez M, *et al*: Guidelines for the use of flow cytometry and cell sorting in immunological studies (second edition). Eur J Immunol 49: 1457-1973, 2019.
31. Robertson B, Dalby AB, Karpilow J, Khvorova A, Leake D and Vermeulen A: Specificity and functionality of microRNA inhibitors. Silence 1: 10, 2010.
32. Livak KJ and Schmittgen TD: Analysis of relative gene expression data using real-time quantitative PCR and the 2(-Delta Delta C(T)) method. Methods 25: 402-408, 2001.
33. Ha M and Kim VN: Regulation of microRNA biogenesis. Nat Rev Mol Cell Biol 15: 509-524, 2014.
34. Landgraf P, Rusu M, Sheridan R, Sewer A, Iovino N, Aravin A, Pfeffer S, Rice A, Kamphorst AO, Landthaler M, *et al*: A mammalian microRNA expression atlas based on small RNA library sequencing. Cell 129: 1401-1414, 2007.
35. Muljo SA, Ansel KM, Kanellopoulou C, Livingston DM, Rao A and Rajewsky K: Aberrant T cell differentiation in the absence of Dicer. J Exp Med 202: 261-269, 2005.
36. Cobb BS, Nesterova TB, Thompson E, Hertweck A, O'Connor E, Godwin J, Wilson CB, Brockdorff N, Fisher AG, Smale ST and Merkenschlager M: T cell lineage choice and differentiation in the absence of the RNase III enzyme Dicer. J Exp Med 201: 1367-1373, 2005.
37. Scherm MG, Serr I, Zahm AM, Schug J, Bellusci S, Manfredini R, Salb VK, Gerlach K, Weigmann B, Ziegler AG, *et al*: miRNA142-3p targets Tet2 and impairs Treg differentiation and stability in models of type 1 diabetes. Nat Commun 10: 5697, 2019.
38. Alharris E, Alghetaa H, Seth R, Chatterjee S, Singh NP, Nagarkatti M and Nagarkatti P: Resveratrol attenuates allergic asthma and associated inflammation in the lungs through regulation of miRNA-34a that targets FoxP3 in mice. Front Immunol 9: 2992, 2018.
39. Kim D, Nguyen QT, Lee J, Lee SH, Janocha A, Kim S, Le HT, Dvorina N, Weiss K, Cameron MJ, *et al*: Anti-inflammatory roles of glucocorticoids are mediated by Foxp3$^+$ regulatory T cells via a miR-342-dependent mechanism. Immunity 53: 581-596.e5, 2020.
40. Perl A: Activation of mTOR (mechanistic target of rapamycin) in rheumatic diseases. Nat Rev Rheumatol 12: 169-182, 2016.
41. Lu LF, Thai TH, Calado DP, Chaudhry A, Kubo M, Tanaka K, Loeb GB, Lee H, Yoshimura A, Rajewsky K and Rudensky AY: Foxp3-dependent microRNA155 confers competitive fitness to regulatory T cells by targeting SOCS1 protein. Immunity 30: 80-91, 2009.
42. Zheng Y, Josefowicz SZ, Kas A, Chu TT, Gavin MA and Rudensky AY: Genome-wide analysis of Foxp3 target genes in developing and mature regulatory T cells. Nature 445: 936-940, 2007.

43. Liu X, Luo M, Meng H, Zeng Q, Xu L, Hu B, Luo Y, Liu C, Luo Z and Yang H: MiR-181a regulates $CD4^+$ T cell activation and differentiation by targeting IL-2 in the pathogenesis of myasthenia gravis. Eur J Immunol: Jul 26, 2019 (Epub ahead of print).
44. Deretic V, Saitoh T and Akira S: Autophagy in infection, inflammation and immunity. Nat Rev Immunol 13: 722-737, 2013.
45. Scheinecker C, Göschl L and Bonelli M: Treg cells in health and autoimmune diseases: New insights from single cell analysis. J Autoimmun 110: 102376, 2020.
46. Rao J, Li S, Wang Q, Cheng Q, Ji Y, Fu W, Huang H, Shi L and Wu X: Comparison of peripheral blood regulatory T cells and functional subsets between ocular and generalized myasthenia gravis. Front Med (Lausanne) 9: 851808, 2022.
47. Kohler S, Keil TOP, Hoffmann S, Swierzy M, Ismail M, Rückert JC, Alexander T and Meisel A: $CD4^+$ $FoxP3^+$ T regulatory cell subsets in myasthenia gravis patients. Clin Immunol 179: 40-46, 2017.
48. Gertel-Lapter S, Mizrachi K, Berrih-Aknin S, Fuchs S and Souroujon MC: Impairment of regulatory T cells in myasthenia gravis: Studies in an experimental model. Autoimmun Rev 12: 894-903, 2013.
49. Song J, Xi JY, Yu WB, Yan C, Luo SS, Zhou L, Zhu WH, Lu JH, Dong Q, Xiao BG and Zhao CB: Inhibition of ROCK activity regulates the balance of Th1, Th17 and Treg cells in myasthenia gravis. Clin Immunol 203: 142-153, 2019.